Nuclear Physics **A518** (1990) 371–388
North-Holland

HIGH-ENERGY PHYSICS WITH POLARIZED ELECTRONS AND MUONS

Vernon W. HUGHES

Yale University, Physics Department, J.W. Gibbs Laboratory, New Haven, CT 06520, USA

Received 22 May 1990
(Revised 17 August 1990)

Abstract: In this paper I will review the topic of high-energy physics with polarized electrons and muons. The two main topics will be the spin-dependent structure functions of the nucleon and parity-violating electroweak interference observed in the scattering of polarized electrons. Both topics now relate to particle physics and to nuclear physics.

1. The SLAC experiment on the proton spin dependent structure function*

It is well known that we can study the structure function of the proton by deep inelastic inclusive ep scattering in which only the outgoing electron is measured. The kinematic variables are Q^2 (4-momentum transfer squared), ν (energy loss) and the dimensionless variable $x = Q^2/2M\nu$, in which M is the proton mass. The proton tensor $W_{\mu\nu}$ involves four independent structure functions $-F_1$ and F_2, which are spin-independent structure functions, and g_1 and g_2, which are spin dependent. In the deep inelastic or scaling regime where Q^2 and ν are large compared to the proton mass, the photon can be considered to act on an individual quark and these functions depend only on the variable x, which can be interpreted as the fraction of the momentum of the proton in the infinite momentum frame that is carried by the struck quark. If both the electron and proton are polarized, we can determine the spin-dependent structure functions from the spin-dependent asymmetries in the differential scattering cross sections. In particular the asymmetry A between the antiparallel and parallel ep-spin cases determines the virtual photon–proton asymmetry A_1 which leads to the spin-dependent structure function g_1. The definitions and relationships are given in eq. (1), where D and η are kinematic factors.

$$A \equiv \left[\frac{\mathrm{d}^2\sigma}{\mathrm{d}\Omega\,\mathrm{d}E'}(\uparrow\downarrow) - \frac{\mathrm{d}^2\sigma}{\mathrm{d}\Omega\,\mathrm{d}E'}(\uparrow\uparrow)\right] \Big/ \left[\frac{\mathrm{d}^2\sigma}{\mathrm{d}\Omega\,\mathrm{d}E'}(\uparrow\downarrow) + \frac{\mathrm{d}^2\sigma}{\mathrm{d}\Omega\,\mathrm{d}E'}(\uparrow\uparrow)\right],$$

$$A = D(A_1 + \eta A_2) \simeq DA_1\,, \qquad g_1(x) = \frac{A_1(x)F_2(x)}{2x(1+R(x))}\,,$$

$$R = \sigma_{\mathrm{L}}/\sigma_{\mathrm{T}}\,. \tag{1}$$

* The review article in ref. [1]) includes a quite complete list of references on this topic.

Further aspects of polarized deep inelastic scattering can be discussed in terms of the absorption of the polarized virtual photon by the polarized proton. For a z-axis collision between a polarized photon and a polarized proton, the total absorption cross section is $\sigma_{3/2}$ for the case of total angular momentum component $+\frac{3}{2}$ and $\sigma_{1/2}$ for total angular momentum component $\sigma_{1/2}$. The asymmetry $A_1 = (\sigma_{1/2}-\sigma_{3/2})/(\sigma_{1/2}+\sigma_{3/2})$ is the virtual photon-proton asymmetry corresponding to the cases of components with total photon and proton angular momentum along the collision axis equal to $\frac{3}{2}$ and $\frac{1}{2}$. At the quark level there is incoherent absorption of the photons by the quarks, and in the absence of orbital angular momentum the virtual polarized photon can be only absorbed when the quark and photon spins are oppositely directed, in order to conserve the component of total angular momentum. A_1 is proportional to the probability that a quark of type i has its spin along the proton-spin direction multiplied by the square of its charge and summed over all types of quarks, or equivalently to the spin-dependent structure function g_1, as given in eq. (2).

$$A_1(x) = \frac{\sum_i e_i^2(q_i^{\uparrow}(x) - q_i^{\downarrow}(x))}{\sum_i e_i^2(q_i^{\uparrow}(x) + q_i^{\downarrow}(x))}, \tag{2a}$$

$$g_1(x) = \tfrac{1}{2}\sum_i e_i^2(q_i^{\uparrow}(x) - q_i^{\downarrow}(x)). \tag{2b}$$

For quark models of the proton $A_1 > 0$.

In 1971 SLAC approved experiment E80 to do the first measurement of polarized deep inelastic ep scattering. The polarized-electron source for this experiment was built at Yale and was based on our atomic physics research at Yale on the production of polarized electrons with an atomic beam (fig. 1). By magnetic deflection in an inhomogeneous magnetic field atoms with a particular component of electronic polarization were selected and photo-ionization of these atoms then led to a source of polarized electrons. The direction of $\boldsymbol{H}$ in the photo-ionization region determines the electron-spin direction, which can therefore be modulated by changing the direction of the current in the large coil. Lithium-6 atoms were chosen for technical reasons and an intense UV flash lamp was used for photo-ionization. The source was installed at SLAC in 1973.

The electron polarization was measured at the injection energy of 70 keV by Mott scattering and at the high-energy output (10–20 GeV) of the linac by Möller scattering by polarized electrons in an iron foil (fig. 2). The analyzing power is large, indeed about 0.8 for 90° scattering in the c.m. system, and the cross section is also large. Because the electron beam from the linac must be deflected about 24° into the experimental area (end station A), the polarization of the beam on the target for a given polarization of the linac output depends on the energy because of the electron g-2 precession. The data agree well with expectation. The operating characteristics of the polarized-electron source (designated PEGGY) are given table 1.

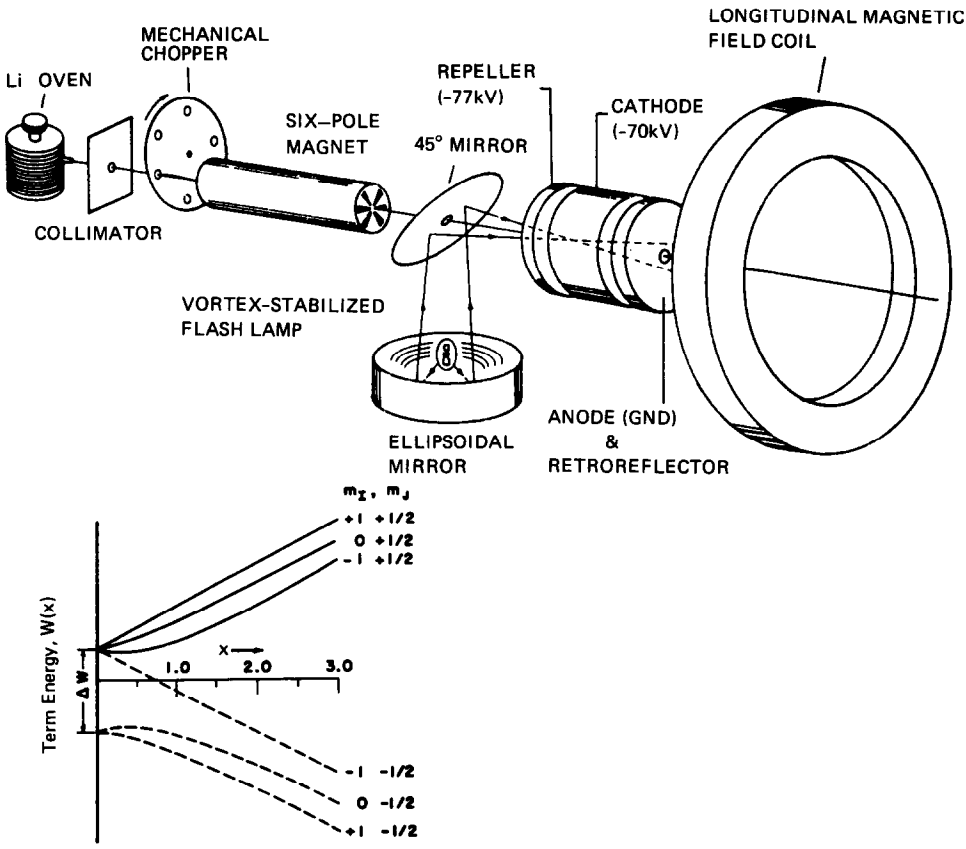

Fig. 1. Schematic diagram of PEGGY showing the principal components of the lithium atomic beam, the uv optics and the ionization region electron optics; Energy level and magnetic moments of ^{6}Li (nuclear spin $I = 1$) in the ground $^2S_{1/2}$ atomic state as a function of magnetic field H.

The polarized-proton target utilized the method of dynamic nuclear polarization with the hydrocarbon butanol and the paramagnetic impurity porphyrexide (fig. 3). At the high field ($B \simeq 5$T) and low temperature ($T \simeq 1$ K) the unpaired electron spins in the porphyrexide are highly polarized according to the Boltzman factor. Due to spin-spin coupling of the electrons and protons, microwave transitions can be driven which transfer the electron polarization to the protons. The target volume was 25 cm^3. The operating characteristics of the target are given in the table 2.

The data for SLAC E80 were taken with the high-resolution 8 GeV/c SLAC spectrometer. Most of the data on polarized electron-proton scattering were obtained in a subsequent experiment, SLAC E130, for which the large acceptance spectrometer shown in fig. 4 was used. This spectrometer consisted of two dipoles, PWC chambers, a gas Cerenkov threshold counter and a Pb glass shower counter. The spectrometer

TABLE 1

Operating characteristics of polarized electron beam

Characteristic	Value
Pulse length	1.5 μs
Repetition rate	180 pps
Average intensity at GeV energies	5×10^8 e^- per pulse
Pulse-to-pulse intensity variation	<5%
Polarization	0.8 ± 0.03
Polarization reversal time	3s
Intensity difference upon reversal	<5%

acceptance $\delta p/p$ was 50%, its resolution $\Delta p/p$ was 1%, and the π^-/e^- rejection factor was 10^{-3}.

The counting rate asymmetry Δ is given by $\Delta = P_e P_p f A$, in which P_e = polarization of electron beam, P_p = polarization of the H-protons in butanol, f = fraction of

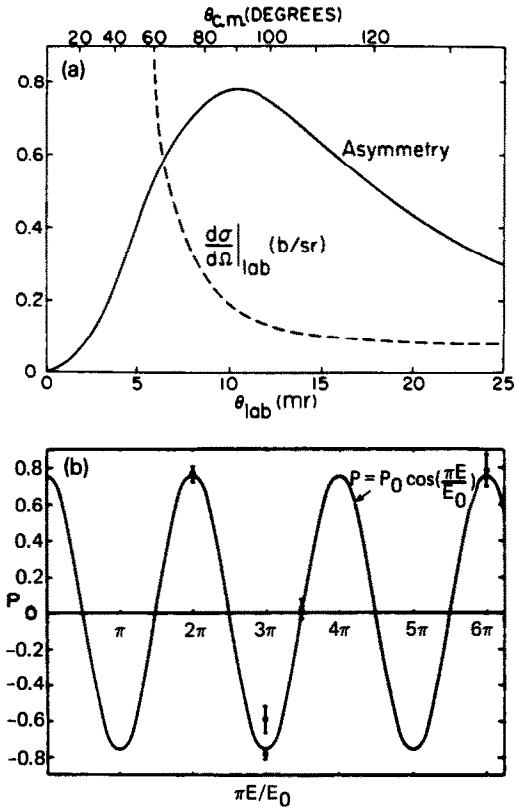

Fig. 2 Measurement of electron beam polarization. (a) The Möller asymmetry and laboratory cross section plotted versus scattering angle for the representative incident energy of 9.712 GeV. (b) The longitudinal component, P, of the beam polarization plotted versus $\pi E/E_0$ with $E_0 = 3.237$ GeV.

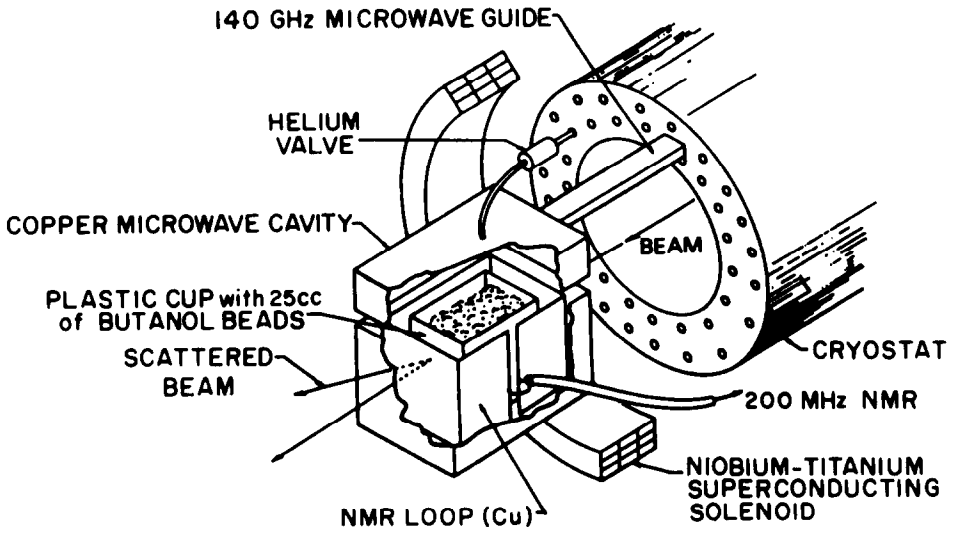

Fig. 3. Schematic diagram of the Yale-SLAC polarized proton target.

nucleons in butanol associated with H, and A = intrinsic ep asymmetry. Since $P_e \approx 0.8$; $P_p \approx 0.6$; $f \simeq 0.1$, the asymmetries Δ are in the range of 0.001 to 0.01 and statistical errors are dominant.

Fig. 5 shows the kinematic range covered which included elastic, resonance region, and deep inelastic scattering. Fig. 6 indicates that A_1^p obeys the scaling relation i.e. it depends only on x and not on Q^2.

There are several important sum rules for spin-dependent structure functions given in eq. (3).

$$S_{Bj} = \int_0^1 dx\,(g_1^p - g_1^n) = \int_0^1 \frac{dx}{2x}\left(\frac{A_1^p F_2^p}{1+R^p} - \frac{A_1^n F_2^n}{1+R^n}\right) = \frac{1}{6}\left|\frac{g_A}{g_V}\right| = 0.209\,(1)\,.$$

TABLE 2

Operating characteristics of polarized proton target

Characteristic	Value
Magnetic field (superconducting)	50 kG
Temperature	1 K
Target material	25 cm^3 of butanol-porphyrexide
Maximum polarization, P_p	0.75
Depolarizing dose $(1/e)^p$	3×10^{14} e^- cm^{-2}
Polarizing time (1/e)	~4 min
Anneal or target change time	~45 min

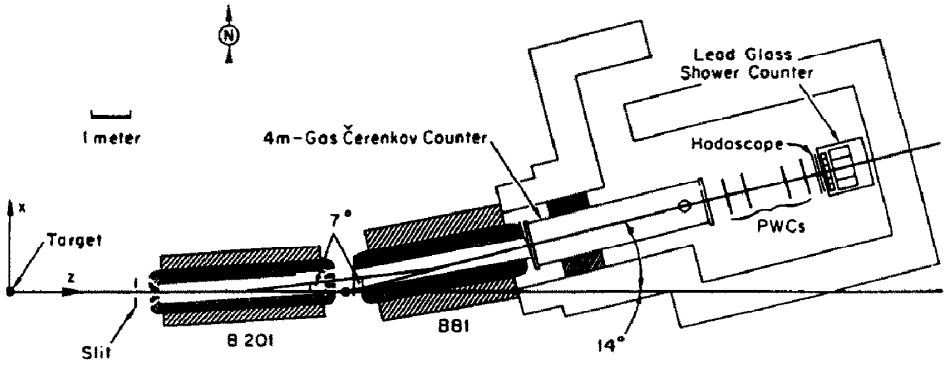

Fig. 4. Electron spectrometer used in SLAC E130 experiment.

With QCD correction

$$S_{\mathrm{Bj}}=\int_0^1 \mathrm{d}x\,(g_1^{\mathrm{p}}-g_1^{\mathrm{n}})=\frac{1}{6}\left|\frac{g_{\mathrm{A}}}{g_{\mathrm{V}}}\right|(1-\alpha_{\mathrm{s}}(Q^2)/\pi)=0.191\,(2)\,,$$

$$S_{\mathrm{EJ}}^{\mathrm{p}}=\Gamma_1^{\mathrm{p}}=\int_0^1 \mathrm{d}x\,g_1^{\mathrm{p}}=\frac{1}{12}\left|\frac{g_{\mathrm{A}}}{g_{\mathrm{V}}}\right|\left[1+\frac{5}{3}\frac{3\mathrm{F/D}-1}{\mathrm{F/D}+1}\right]+\mathrm{O}(\alpha_{\mathrm{s}})=0.189\pm0.005\,,$$

$$S_{\mathrm{EJ}}^{\mathrm{n}}=\Gamma_1^{\mathrm{n}}=\int_0^1 \mathrm{d}x\,g_1^{\mathrm{n}}=\frac{1}{12}\left|\frac{g_{\mathrm{A}}}{g_{\mathrm{V}}}\right|\left[-1+\frac{5}{3}\frac{3\mathrm{F/D}-1}{\mathrm{F/D}+1}\right]+\mathrm{O}(\alpha_{\mathrm{s}})=-0.002\pm0.005\,, \qquad (3)$$

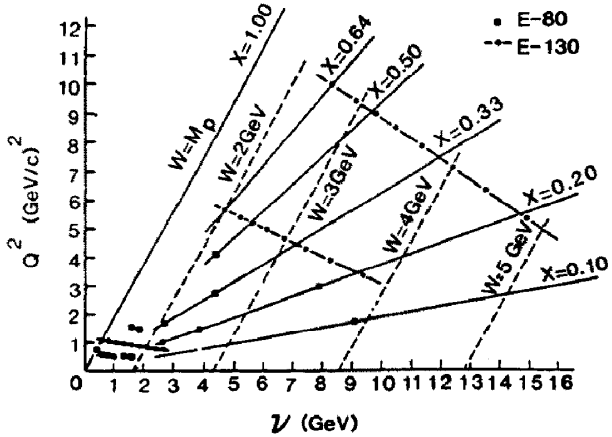

Fig. 5. Kinematic points measured.

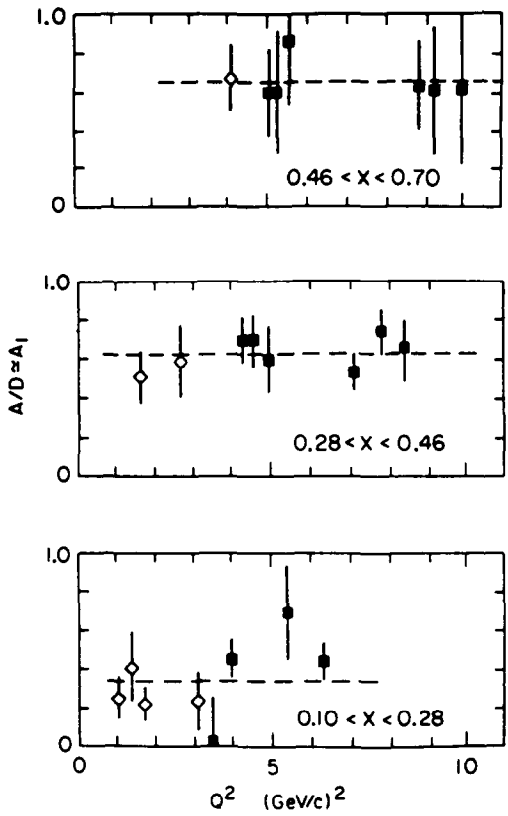

Fig. 6. Radiatively corrected values of $A/D \simeq A_1$ obtained in SLAC E80 (open diamonds) and in SLAC E130 (closed squares) plotted vs Q^2. The fits to horizontal lines demonstrate scaling of A_1.

where

$$g_1 = \frac{A_1 F_2}{2x(1+R)}, \qquad g_A = 1.254\,(6), \qquad R = \frac{\sigma_L}{\sigma_T},$$

$$\alpha_s = 0.27\,(2) \qquad \text{at} \qquad Q^2 = 11\ (\text{GeV}/c)^2,$$

$$F/D = 0.631 \pm 0.018\,.$$

The Bjorken polarization sum rule is a basic relation, originally derived from current algebra for a quark model of the nucleon and with incorporation of the view, now well established, that the weak interactions of quarks and leptons are the same. This remarkable relation between structure functions and constants characterizing nuclear beta decay was derived in 1966 and played a seminal role in stimulating our experimental program. This sum rule can be derived in the quark-parton model by evaluating the expectation value of the axial vector beta decay operator for n→p decay. It is now recognized as a rigorous consequence of QCD in the scaling limit and the $O(\alpha_s)$ correction has been computed by perturbative

QCD. First moments of the spin-dependent structure functions for proton and neutron separately were given by Ellis and Jaffe. These sum rules are model dependent, with the principal assumption being that the strange quark sea is unpolarized.

The measured values of A_1^p are shown in fig. 7. At low x, where the scattering is expected to be predominantly by unpolarized sea quarks, A_1^p is small. As x increases, scattering by the valence quarks which should carry the spin of the proton becomes more important and A_1^p increases. Indeed as $x \to 1$, perturbative QCD predicts that $A_1^p \to 1$ since the struck quark should carry the entire spin of the proton. A test of the Ellis-Jaffe sum rule can be made with these data. The value obtained for the first moment of the proton spin dependent structure function is

$$\Gamma_1^p = \int_0^1 g_1^p(x)\,dx = 0.17 \pm 0.05\,. \tag{4}$$

The error in the experimental value is relatively large because the data only extend down to $x = 0.1$ and hence a large extrapolation is required to determine the first moment of g_1. Agreement between experiment and theory is satisfactory within the experimental error.

Comparison of the data with various theoretical models is shown in fig. 8. Best agreement is obtained with the quark model of Carlitz and Kaur. It is an unsymmetrical model which satisfied the Ellis-Jaffe sum rule, Regge theory at low x, perturbative QCD at high x and includes an adjustable parameter to account for the transfer of the spin of valence quarks to sea quarks.

2. The SLAC-Yale parity-nonconservation experiment

In 1972 when we were developing the polarized electron source at Yale for our approved SLAC experiment E80 to study the spin-dependent structure function of

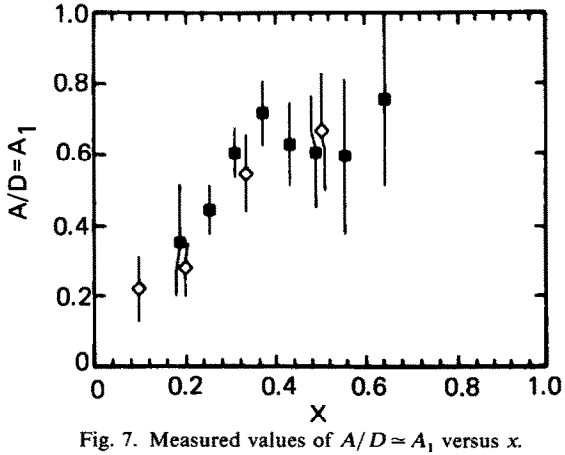

Fig. 7. Measured values of $A/D = A_1$ versus x.

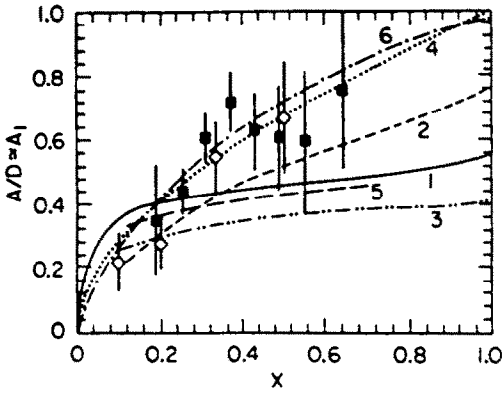

Fig. 8. Experimental values A_1 compared with theories. 1 - Symmetrical valence-quark model. 2 - Current quarks. 3 - Orbital angular momentum. 4 - Unsymmetrical model. 5 - MIT bag model. 6 - Source theory.

the proton, Prescott of SLAC proposed that we test parity conservation in deep inelastic electron scattering with our polarized electron source by looking for a helicity dependence of the differential scattering cross section [2,3]). The motivation for this proposal was to search for an electromagnetic interaction involving a new neutral axial vector electromagnetic current. No weak interaction or electroweak interference was mentioned. Actually, as is now well known, the real motivation turned out to be very strong when in 1973 neutral currents were discovered, and then establishing electroweak interference became urgent. The Feynman diagrams of fig. 9 illustrate that scattering can occur either through γ or Z exchange. Parity nonconservation would be indicated by a pseudoscalar term with $\boldsymbol{\sigma}_e \cdot \boldsymbol{p}_e$ in which $\boldsymbol{p}_e$ = incident electron momentum and $\boldsymbol{\sigma}_e$ = electron spin. Eq. (5) gives the relevant relations

$$d\sigma^{+(-)} \propto |M_{e.m.} + M_W^{+(-)}|^2 , \qquad A = \frac{d\sigma^+ - d\sigma^-}{d\sigma^+ + d\sigma^-} ,$$

$$|A| \simeq \frac{M_{e.m.} M_W}{M_{e.m.}^2} \simeq \frac{Q^2}{M_Z^2} \simeq \frac{G_F Q^2}{4\pi\alpha} , \qquad |A| \simeq (10^{-5}\text{–}10^{-4}) \frac{Q^2}{M_p^2} . \tag{5}$$

The scattering cross section is the square of the sum of these amplitudes. If weak Z-exchange is parity violating, then the interference term should contribute a helicity dependence to $d\sigma$. This term is of relative order $A_{weak}/A_{e.m.}$ and would be expected to have the magnitude indicated. Most impressively, Zeldovich [4]) had suggested this experiment and viewpoint in 1959, as well as the atomic bismuth PNC experiment. None of us at SLAC or Yale were aware of his proposal.

The first PNC experiment was done with the PEGGY I beam, first as a byproduct of E80 [5]) and then in a separate dedicated experiment E95 [6]). However, the intensity of the polarized electron beam from PEGGY I was too small and the asymmetry level of only 10^{-3} was attained. Wilson of Harvard proposed using a large-solid-angle spectrometer for backward scattering using the PEGGY beam. But the experiment

Fig. 9. Feynman diagrams indicating a cross section asymmetry A between + and − helicity polarized electrons scattered from unpolarized protons. The asymmetry arises from interference between the electromagnetic amplitude $M_{e.m.}$ associated with γ exchange and the weak amplitude M_W associated with Z exchange. M is the proton mass in GeV and Q^2 is the 4-momentum transfer squared in $(\mathrm{GeV}/c)^2$.

actually done at SLAC, E122, involved the development of a new high intensity source of pulsed polarized electrons (PEGGY II). This was based on photoemission of valence electrons from the semiconductor GaAs by polarized laser light (fig. 10). The operating characteristics are given in the accompanying table 3.

The experimental setup is shown in fig. 11. A liquid deuterium target was used because its nucleon density is greater than that of liquid hydrogen and D is an isoscalar nucleus. The spectrometer consisted of two bending magnets and a quadrupole magnet. Both an N_2 gas threshold counter and a Pb glass shower counter were used to detect scattered electrons and discriminate against pions. Because of the high counting rates both detectors were used in an integrating mode. To avoid helicity dependence of the characteristics of the polarized electron beam - its position, angle and energy - extensive measurements of the linac output beam were made with beam position monitors. This information was used in a computer controlled feedback system to control the beam (fig. 12).

Fig. 13 shows the ed scattering cross section and the spectrometer acceptance. The scattering observed was predominantly in the deep inelastic regime.

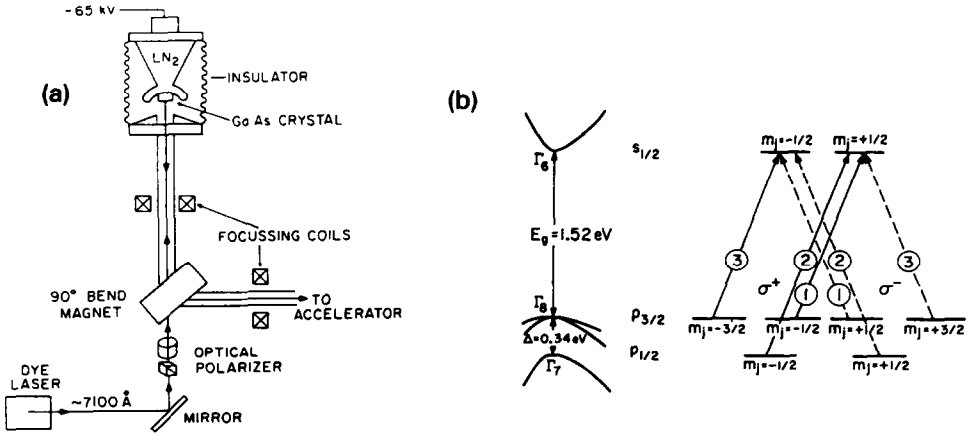

Fig. 10. (a) Schematic diagram of PEGGY II, showing the GaAs crystal in the electron gun and the laser optics. (b) Energy bands of GaAs at the Γ point (left) and transitions between the $S_{1/2}$ levels and the $P_{1/2}$ and $P_{3/2}$ levels. Solid (broken) lines indicate transitions for $\sigma^+(\sigma^-)$ light, and the circled numbers indicate the relative transition strengths. Operating characteristics shown in the table 3.

TABLE 3
PEGGY II operating characteristics

Characteristic	Value
Pulse length	1.5 μs
Repetition rate	120 pps
Electron intensity (at high energy)	(1 to 4) × 10^{11} e^-/pulse
Pulse to pulse intensity variation	~3%
Electron polarization	0.37, average
Polarization reversal time	pulse to pulse

Fig. 14 shows the experimental results. The measured asymmetry versus the beam polarization is shown, where as indicated earlier (fig. 2a) the beam polarization on the target in end station A depends on energy due to the electron g-2 spin precession. The measured asymmetry values are given below for ed and also for ep scattering.

$$e^- + D \to e^- + X \text{ (DIES)},$$

$$\frac{A}{Q^2} = (-9.5 \pm 1.6) \times 10^{-5} \text{ (GeV/}c\text{)}^{-2},$$

$$[\text{Statistical error} = 0.86 \times 10^{-5}] \qquad [\text{Systematic error} \simeq 0.7 \times 10^{-5}],$$

$$\langle Q^2 \rangle = 1.6 \text{ (GeV/}c\text{)}^2 \qquad \langle y \rangle = \nu / E_0 = 0.21, \tag{6a}$$

$$e^- + P \to e^- + X \text{ (DIES)},$$

$$\frac{A}{Q^2} = (-9.7 \pm 2.7) \times 10^{-5} \text{ (GeV/}c\text{)}^{-2},$$

$$[\text{Statistical error} = 1.6 \times 10^{-5}], \qquad [\text{Systematic error} = 1.1 \times 10^{-5}],$$

$$\langle Q^2 \rangle \simeq 1.6 \text{ (GeV/}c\text{)}^2, \qquad \langle y \rangle = 0.21. \tag{6b}$$

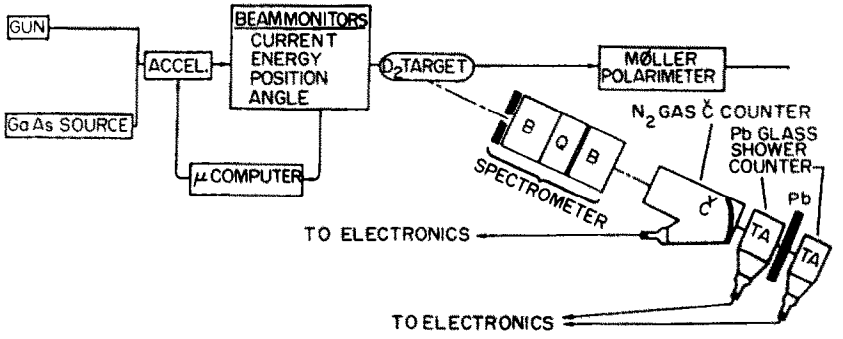

Fig. 11. Block diagram of the apparatus used to detect parity nonconservation in deep inelastic scattering of polarized electrons.

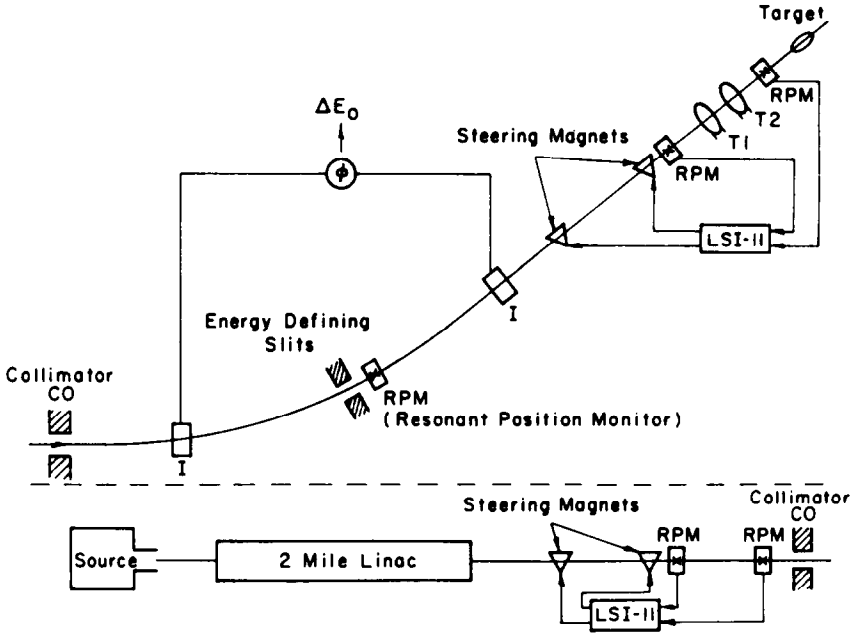

Fig. 12. Detail of the beam monitoring system, including resonant position monitors, ΔE monitor, and toroids T_1 and T_2.

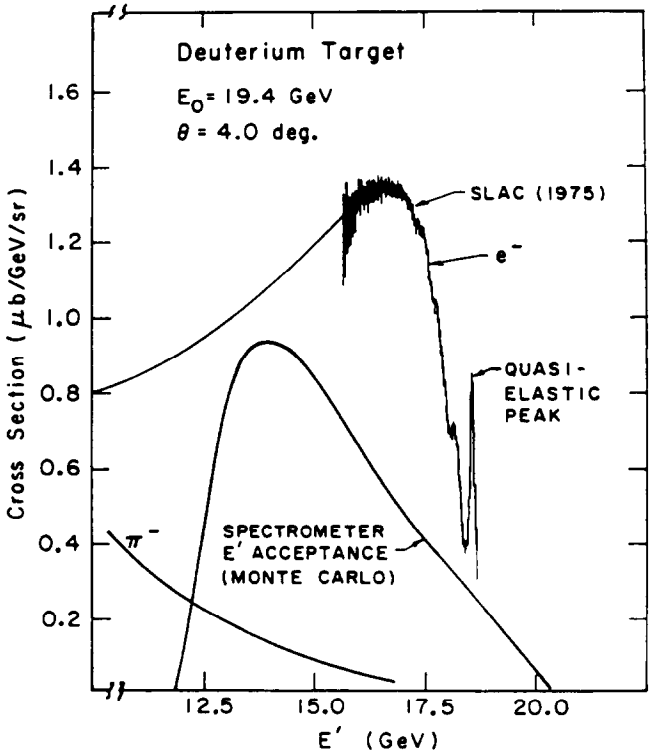

Fig. 13. Acceptance of the high rate spectrometer used for the parity nonconservation experiment.

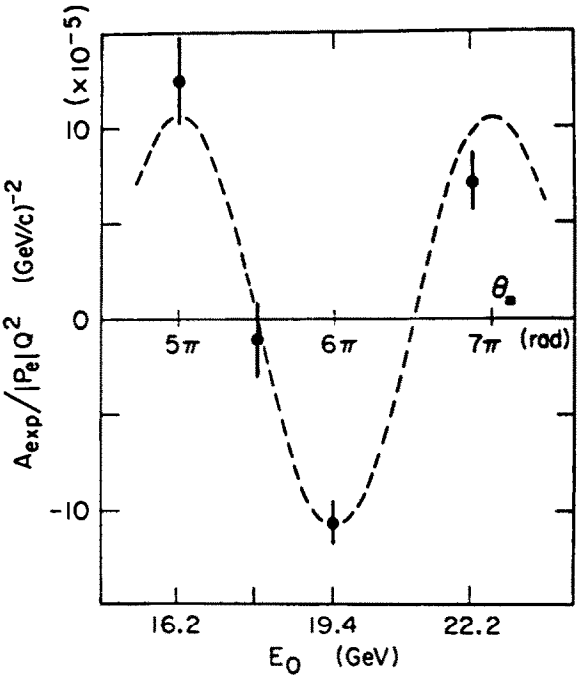

Fig. 14. Experimental asymmetry as a function of beam energy. Broken line was calculated assuming that the theoretical asymmetry is independent of energy but that the beam helicity changes in the 24.5° bending magnet due to the g-2 precession.

This experimental result was the first unambiguous observation of electroweak interference and did much to establish the unified electroweak theory. The value obtained for $\sin^2\theta_W$ is

$$\sin^2\theta_W = 0.221 \pm 0.015 \pm [0.013]_{\text{(theor.)}}. \tag{7}$$

3. The parity-nonconservation experiment at Bates

Another electroweak interference experiment based on the same principle was recently completed at the Bates electron linac laboratory. In 1975 Feinberg suggested [7]) that electroweak interference might be usefully studied in the scattering of polarized electrons by nuclei at relatively low momentum transfer. In particular he suggested that for elastic scattering from a spin zero, isoscalar nucleus such as ^{12}C, the asymmetry would not depend on the nuclear form factor and could cleanly test the unified electroweak theory. The relation between the asymmetry and the electroweak parameters is given in eq. (8).

$$A = \frac{\sigma_R - \sigma_L}{\sigma_R + \sigma_L} = \tilde{\gamma}\frac{3}{2}\frac{G_F Q^2}{\sqrt{2}\pi\alpha} = 4\times 10^{-4}\frac{Q^2}{M_p^2}\sin^2\theta_W. \tag{8}$$

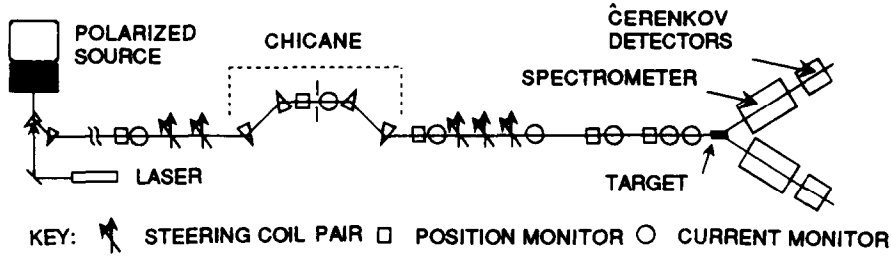

Fig. 15. Schematic diagram of the Bates parity nonconservation experiment which measured helicity-dependent elastic scattering of polarized electrons by ^{12}C.

The experimental arrangement is shown in fig. 15. The polarized electron source, built at Yale [8]), was based on photo-emission from GaAs by polarized laser light. The duty factor was about 1% and the average current was 30–60 μA. The energy of the electron beam was 250 MeV and Q^2 was 0.02 $(\mathrm{GeV}/c)^2$. A pair of quadrupole spectrometers and integrating Cerenkov detectors were used.

The measured asymmetry was small, $A = 0.56 \pm 0.14$ ppm, and the error is dominantly due to limited statistics. A value for the isoscalar vector hadronic coupling constant $\tilde{\gamma}$ was determined [9]). The result also determines $\sin^2\theta = 0.202 \pm 0.049$. The values are consistent with the standard theory [10]).

4. The CERN polarized muon–proton scattering experiment*

Finally we review briefly the recent CERN experiment by the EMC group on the measurement of the proton-spin-dependent structure function using a high-energy polarized muon beam. We will also mention future plans at CERN for further measurements of the spin-dependent structure functions of both the proton and the neutron.

The experimental setup is shown in fig. 16 with the polarized-proton target, the EMC forward spectrometer and the incident polarized muon beam. The muon beam energy was between 100 and 200 GeV, and principally inclusive scattering was studied. The EMC polarized target is shown in fig. 17. This enormous target used irradiated NH_3 as the target material. Shown in table 4 are the projected operating conditions for a modified target with a hydrocarbon as the target material to be used in a new experiment by the spin muon collaboration (SMC).

The virtual photon-proton asymmetry A_1^p determined from the measured asymmetries are shown in fig. 18 together with the SLAC data points. In the region of

* Ref. [11]) includes a quite complete list of references on this topic.

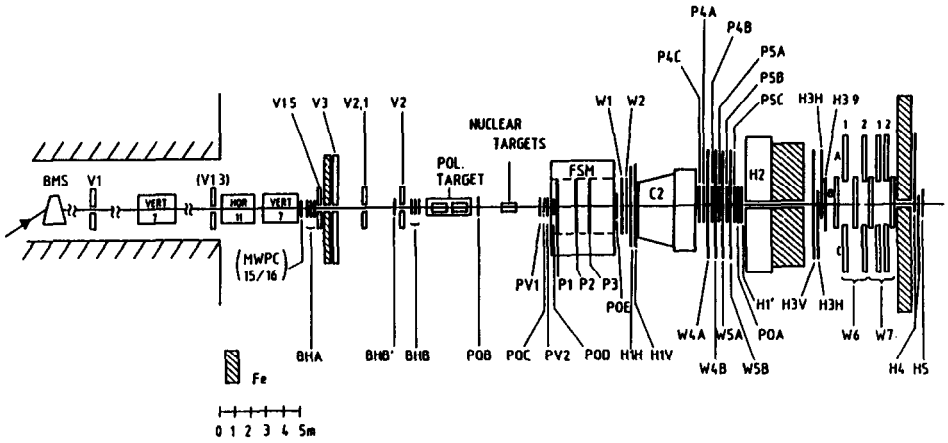

Fig. 16. The EMC forward spectrometer for the CERN EMC polarized-target experiment.

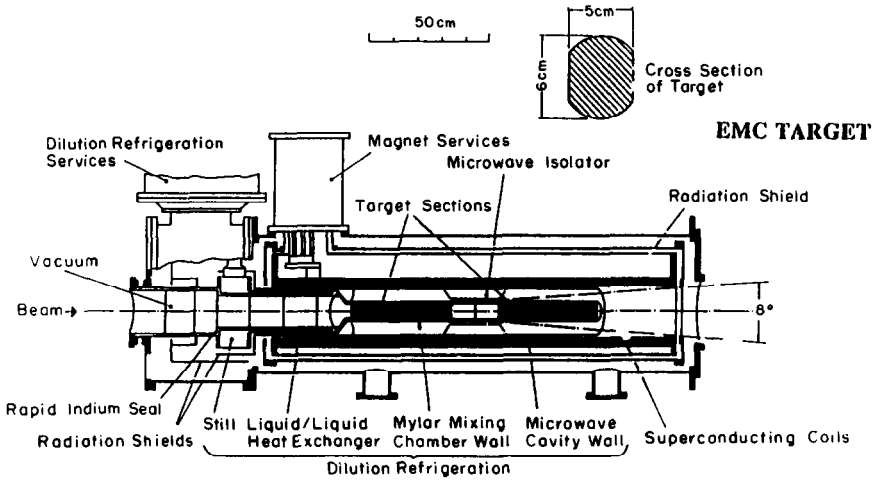

Fig. 17. The EMC polarized target.

TABLE 4

Projected operating conditions for SMC polarized target

Target material	Butanol and deuterated butanol (Doped with EHBA-Cr (V))
Magnet field	2.5 T
Temperature	0.5 K for DNP mode
	0.05 K for frozen spin mode
Polarization	0.8 for proton; 3% rel. error
	0.4 for deuteron; 3% rel. error

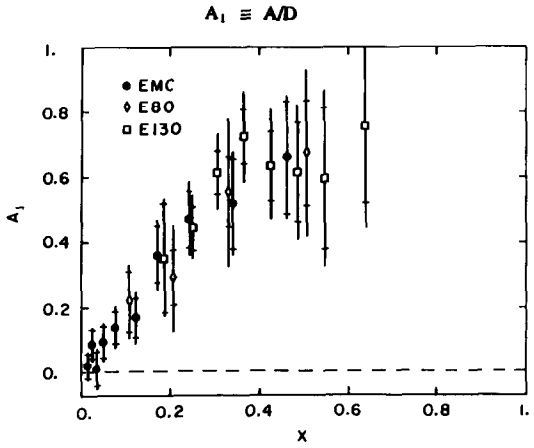

Fig. 18. Compilation of all the data of A_1^p as a function of x. The EMC points are shown as full circles while the SLAC points are shown as open diamonds (experiment E80) and open squares (E130). Inner error bars are the statistical errors and the outer error bars are the total errors (statistical plus systematic added in quadrature). The systematic errors include uncertainties in the values of R and A_2.

overlap the EMC and the SLAC data agree well. The principal contribution of the CERN data is to determine A_1 to lower values of x, indeed down to $x = 0.01$. This is a very important contribution because it allows a much more sensitive test of the Ellis-Jaffe sum rule as indicated in fig. 19. The conclusion is that the data disagree with the Ellis-Jaffe sum rule.

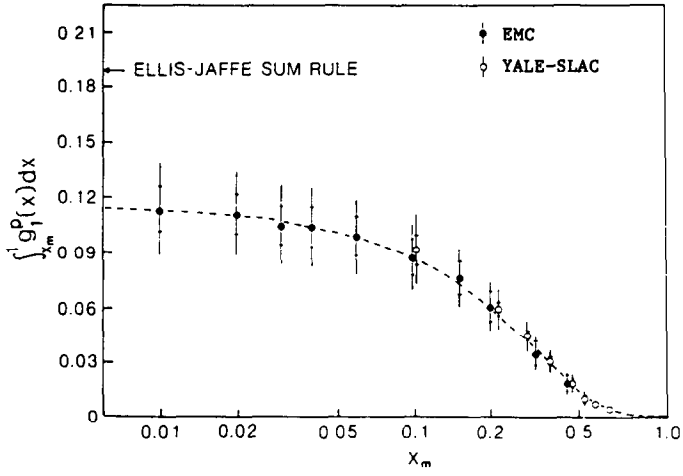

Fig. 19. The value of the integral $\int_{x_m}^{1} g_1^p \, dx$ as a function of x_m, the value of x at the low edge of each bin.

The implication based on the naive quark-parton model is that very little of the proton spin is contributed by the quark spins. This surprising conclusion has attracted great interest and has led to many theoretical papers. Possible reasons for the discrepancy and mechanisms by which gluons or orbital angular momentum could contribute to the proton spin have been discussed extensively.

The present high interest in the nucleon-spin-dependent structure functions has led to plans for new experiments. In particular, a new collaboration at CERN (SMC) will do CERN experiment NA47 [12]) to measure the neutron-spin-dependent structure function and also to improve knowledge of A_1^p. This should allow a test of the fundamental Bjorken polarization sum rule. In addition, an experiment is planned at HERA to use the electron ring with an internal polarized H or D gas target to measure A_1^p and A_1^n. Also an experiment has been approved at SLAC to use a polarized ^{3}He target to measure A_1^n.

A summary of the present situation and a listing of some important experimental and theoretical problems is given below.

EMC(CERN) data on polarized μ-p DIS extended SLAC polarized ep data to $x \cong 0.01$; CERN and SLAC data agree from $x = 0.1$ to 0.7:

(i) Violation of Ellis-Jaffe sum rule for Γ_1^p.

(ii) If the Bjorken sum rule is valid, the implication is that A_1^n and Γ_1^n are much larger than previously predicted.

(iii) According to interpretation with naive quark-parton model, quark spin seems to carry very little of the proton spin.

Important experimental problems:

(i) Measure A_1^n, Γ_1^n for the first time and improve data on A_1^p and Γ_1^p;

(ii) If the Bjorken sum rule is valid, the implication is that A_1^n and Γ_1^n are much larger than previously predicted.

(iii) According to interpretation with naive quark-parton model, quark spin seems to carry very little of the proton spin.

Important experimental problems:

(i) Measure A_1^n, Γ_1^n for the first time and improve data on A_1^p and Γ_1^p; Particularly to test the Bjorken polarization sum rule;

(ii) Measure A_2^p and A_2^n;

(iii) Measure spin-dependent effects in exclusive channels, e.g. (J/Ψ).

Theoretical problems:

(i) Ellis-Jaffe sum rule;

(ii) Carriers of proton spin;

(iii) Nucleon spin dependent structure functions.

Implications:

(i) Polarized hadron–hadron scattering;
(ii) Parity violation in atoms;
(iii) Dark matter in universe.

It is quite clear that the subject of the nucleon spin dependent structure functions is a rich and active one.

This paper was adapted from the lecture given on the occasion of the award of the 1990 Bonner Prize in Nuclear Physics by the American Physical Society. The discussion emphasizes those aspects of the topics in which Yale physicists were involved.

I am most pleased to be able to contribute this paper in honor of and on the happy occasion of Torleif Ericson's 60th birthday. For many years I have been fortunate to be a friend of Torleif's. Often our scientific interests have overlapped and I have learned a great deal from Torleif. For the past few years together with Darragh Nagle we have worked on a book entitled "*The meson factories*" which was just submitted for publication to the University of Califnoria Press in their Los Alamos Series. The topic of this paper "High Energy Physics with Polarized Electrons and Muons" relates to both particle physics and nuclear physics and in this respect illustrates well the focus of interest of much of Torleif's work.

Research supported in part by the Department of Energy under Contract No. DE-AC02-76-ER03075.

References

1) V.W. Hughes and J. Kuti, Ann. Rev. Nucl. Part. Sci. **33**, (1983) 611
2) C.Y. Prescott *et al.*, Phys. Lett. **B77** (1978) 347
3) C.Y. Prescott *et al.*, Phys. Lett. **B84** (1979) 524
4) Y.B. Zel'dovich, Sov. Phys. JETP **36** (1959) 682
5) M.J. Alguard *et al.*, Phys. Rev. Lett. **37** (1976) 1261
6) W.B. Atwood *et al.*, Phys. Rev. **D18** (1978) 2223
7) G. Feinberg, Phys. Rev. **D12** (1975) 3575
8) G.D. Cates *et al.*, Nucl. Instr. Meth. **A278** (1989) 293
9) P.A. Souder *et al.*, Phys. Rev. Lett. **65** (1990) 694
10) P.Q. Hund and J.J. Sakurai, Ann. Rev. of Nucl. and Part. Sci. **31** (1981) 375
11) J. Ashman *et al.*, Nucl. Phys. **B328** (1989) 1
12) V.W. Hughes (SMC spokesman) Measurement of the spin-dependent structure functions of the neutron and proton, 12/22/88, CERN Experiment NA47